

Research Article

Aldias Bahatmaka*, Andi Abdullah Ghyferi, Samsudin Anis, Deni Fajar Fitriyana, Rahmat Doni Widodo, Sang Won Lee, Joung Hyoung Cho, Teguh Muttaqie, Januar Parlaungan Siregar, Tezara Cionita, Janviter Manalu, and Achmad Yanuar Maulana

The topology optimization applied to the evaluation study of bracket caliper by using finite element method

<https://doi.org/10.1515/cls-2025-0036>

received November 04, 2024; accepted August 09, 2025

Abstract: The purpose of this article is to analyze the deformation, equivalent elastic strain, and safety factor of a bracket. The research applies a numerical study of topology optimization of evaluation for the structures by using a finite element analysis (FEA) and using aluminum alloy 6061 T6 and cast iron EN GJL 100 materials. The benchmarking of mesh condition by comparing the result with the reference's data is in good agreement, with error correction less than 5%. On the other hand, the results of the bracket evaluation show that aluminum alloy is more elastic and durable than cast iron. However, cast iron has a higher safety factor than aluminum alloy. The safety factor indicates the structural integrity of a certain material by limiting the maximum force that may be applied. The FEA and optimization results showed that the

optimization reduced deformation by 15%. Strain decreased by 21% after optimization. Stress experienced a 25% reduction due to optimization. In this specific topology, weight reduction occurs consistently, resulting in a 31% decrease. This means the topology optimization is effective to evaluate the design structure, such as the bracket caliper, and also shows the reduction in iteration time when the finite element method is applied.

Keywords: topology optimization, bracket caliper, design structure, finite element method

1 Introduction

Finite element analysis (FEA), which was originally developed for aircraft structural analysis, is now widely utilized in a variety of sectors, including automotive [1–3], structural engineering [4–7], composite design and production [8–10], and medical [11–13]. The caliper bracket offers unorthodox accuracy and lies, allowing the user to achieve precise scoring dimensions and ensure a proper seal. Versatile design and integration of advanced technologies help it perform its functions more effectively, making it essential when ensuring the quality, reliability, and security of many applications.

The static analysis of the bracket caliper is an important feature. Static analysis examines how the bracket caliper behaves structurally under various loads and circumstances. In research on the FEA of an ammo bracket, the stress distribution under working load was calculated, and the stress was modified using the Goodman theory approach to forecast the fatigue life and safety factor of the bracket [14]. Engineers can evaluate the performance of the caliper and spot any possible problem areas by putting them under a variety of loads, such as axial, bending, or torsional forces. Engineers may enhance the strength, rigidity, and stability of bracket caliper using static

* Corresponding author: Aldias Bahatmaka, Department of Mechanical Engineering, Universitas Negeri Semarang, Gunungpati, Semarang 50229, Indonesia, e-mail: aldiasbahatmaka@mail.unnes.ac.id

Andi Abdullah Ghyferi, Samsudin Anis, Deni Fajar Fitriyana, Rahmat Doni Widodo: Department of Mechanical Engineering, Universitas Negeri Semarang, Gunungpati, Semarang 50229, Indonesia

Sang Won Lee: Department of Fluid, Research and Development, Daewoo Shipbuilding and Marine Engineering, Co. Ltd., Geoje 53305, South Korea

Joung Hyoung Cho: Interdisciplinary Program of Marine Design Convergence, Pukyong National University, Busan 48513, South Korea

Teguh Muttaqie: Research Center for Hydrodynamics Technology, BRIN, Surabaya 60117, Indonesia

Januar Parlaungan Siregar: Centre for Automotive Engineering (Automotive Centre), Universiti Malaysia Pahang Al-Sultan Abdullah (UMPSA), Pekan 26600, Pahang, Malaysia

Tezara Cionita: Faculty of Engineering and Quantity Surveying, INTI International University, Nilai 71800, Malaysia

Janviter Manalu: Faculty of Engineering, Universitas Cenderawasih, Kota Jayapura 99358, Indonesia

Achmad Yanuar Maulana: Department of Chemistry, Dong-A University, Busan, 49315, South Korea

analysis, which will also increase their overall performance and lifetime.

The definition of a safety factor varies depending on the situation. For instance, in geomechanics issues, the second-order work criteria under local and global forms are specified as an appropriate safety factor [15]. The reliability and safety of bracket caliper must be determined not only via static analysis but also through the examination of stress and safety factors. When an object is subjected to tension, it will change in shape, either lengthening or shrinking, due to the presence of a load or stress [16]. Calculating the maximum stress that caliper parts like the bracket arm and measuring jaws would encounter under various load circumstances is called stress analysis. This study aids in locating locations of concentrated high stress that could need design alterations or reinforcement. Additionally, the safety factor is derived by dividing the ultimate strength of the material by the highest amount of stress. A higher safety factor denotes more dependability and safety. Engineers can reduce the danger of damage or injury during operation by doing stress analysis and analyzing the safety factor to make sure that bracket caliper can bear the anticipated loads without failing.

This study shows a new way to use topology optimization and FEA together to design a bracket caliper using two different types of engineering materials. There are other studies like this one, but this one is the only one that compares mesh convergence with verified external data, measures how well materials work under realistic loads, and uses structural optimization to make motorcycle braking systems work better in the real world. This work is new because it uses a multi-criteria approach to evaluate performance and choose materials.

2 Previous research on numerical optimization

Numerical optimization enhances aeronautical applications by decreasing weight, boosting structural stability and efficiency, and lowering operational costs [17]. Numerical optimization plays a pivotal role in the evolution of topology optimization, providing robust mathematical frameworks to design efficient, innovative, and high-performance structures. Over the last decade, extensive research

Table 1: Summary of the review study on numerical optimization

Author [refs]	Optimization subject	Description	Conclusion
Andreozzi and Davino [18]	This research focuses on topological sensitivity analysis, a part of structural optimization. Its aim is to identify crucial parts of a design that significantly impact its structural performance	The method employs analytical approaches to compute sensitivity derivatives with respect to changes in topology. This information guides the optimization process to modify the structure in the most effective manner	The article concludes that topology optimization for sustainable design can lead to reduced carbon footprints and improved sustainability of products and processes
Guo and Liu [19]	This research discusses topology optimization considering manufacturing constraints, particularly applicable to additive manufacturing applications such as 3D printing	The method integrates geometric and manufacturing process constraints into the topology optimization process. This ensures that the designs generated can be manufactured using specific additive manufacturing techniques without difficulty	The study shows that topology optimization considering manufacturing constraints can produce designs that are easier to produce using additive manufacturing technologies
Liu and Zhang [20]	This research focuses on topology optimization considering structural integrity constraints, crucial to prevent structural failure in designs	The method integrates strength and stiffness constraints into the topology optimization process. This ensures that the resulting designs are not only structurally optimal but also maintain necessary structural integrity	The study concludes that integrating structural integrity constraints into topology optimization results in more reliable and structurally safe designs
Zhou and Wang [21]	This research explores topology optimization for sustainable design, considering environmental impacts of materials and production processes	The method integrates life cycle analysis and carbon footprint assessment into topology optimization. This allows for designs that are not only structurally optimal but also environmentally sustainable	The article concludes that topology optimization for sustainable design can lead to reduced carbon footprints and improved sustainability of products and processes

has explored various aspects of numerical optimization, addressing complex challenges such as structural integrity, material behavior, manufacturing constraints, and sustainability. This synthesis reviews eight recent studies that highlight the integration of numerical optimization techniques in topology optimization, showcasing the progression from traditional methods to advanced, multi-faceted approaches shown in Table 1. These studies offer a comprehensive understanding of how numerical optimization can be effectively applied to develop optimal and reliable topological designs across a spectrum of engineering disciplines.

3 Theoretical basis

3.1 Material properties

In this model, two types of materials, namely aluminum alloy, wrought, 6061 T6 and cast iron EN GJL 100 [22], were used. Based on the material's unique characteristics as shown in Table 2, both options were chosen. Due to its exceptional qualities in structural and industrial applications, aluminum alloy, wrought, 6061 T6 is used. High strength and good corrosion resistance are two qualities

of this material. It is appropriate for usage in a range of applications, including engine components, cars, and airplanes because of its great strength and comparatively lighter weight.

Cast iron EN GJL 100 is further used as a comparative material. Due to its special worn out of resistance, high strength, and dimensional stability features, this material was selected. These materials are frequently utilized in applications like engine blocks, brake parts, and wheels that need high pressure and friction resistance. To compare the effectiveness of these two materials, this benefit is thought to be a viable option for this study. Before being employed in study, both materials were properly prepared with the following material characteristics.

3.2 Design

Autodesk Inventor was utilized to perform the initial design work. Combining the dimensions, a side view of the caliper mount was created to get an initial design documented. Figure 1 shows the first sketch of the brake and caliper mount. Once the caliper mount was dimensioned, Autodesk Inventor was utilized to create a 3D model of the motorcycle's

Table 2: Material properties

Aluminum alloy, wrought, 6061 T6		Cast iron EN GJL 100	
Mechanical properties	Metric	Mechanical properties	Metric
Density	2.7 g/cc	Density	5.54–7.81 g/cc
Hardness, Brinell	95	Hardness, Brinell	110–807
Hardness, Knoop	120	Hardness, Knoop	162–906
Hardness, Rockwell A	40	Hardness, Rockwell B	40.0–800
Hardness, Rockwell B	60	Hardness, Rockwell C	11.4–65.0
Hardness, Vickers	107	Hardness, Vickers	151–871
Ultimate tensile strength	310 MPa	Tensile strength, ultimate	90.0–1,650 MPa
Tensile yield strength	276 MPa	Tensile strength, yield	65.5–1,450 MPa
Elongation at break	12%	Elongation at break	0.200–40.0%
Elongation at break	17%	Reduction of area	2.00–10.0%
Modulus of elasticity	68.9 GPa	Modulus of elasticity	62.1–250 GPa
Notched tensile strength	324 MPa	Flexural yield strength	248–655 MPa
Ultimate bearing strength	607 MPa	Compressive yield strength	220–2520 MPa
Bearing yield strength	386 MPa	Poisson's ratio	0.240–0.370
Poisson's ratio	0.33	Fatigue strength	68.9–510 MPa
Fatigue strength	96.5 MPa	Fracture toughness	44.0–110 MPa m ^{1/2}
Fracture toughness	29 MPa m ^{1/2}	Machinability	0.00–125%
Machinability	50%	Shear modulus	27.0–67.6 GPa
Shear modulus	26 GPa	Shear strength	149–1,480 MPa
Shear strength	207 MPa	Izod impact unnotched	4.00–244 J
		Charpy impact	0.100–40.0 J
		Charpy impact, unnotched	2.70–200 J

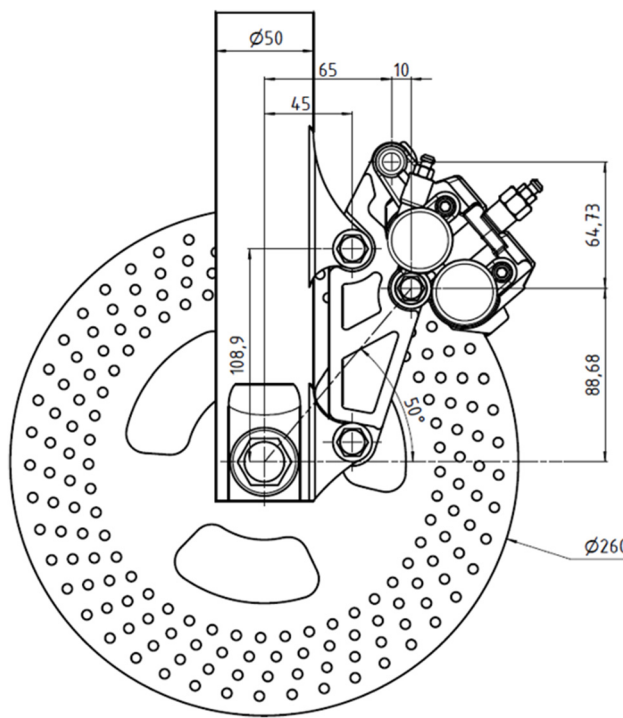


Figure 1: Sketch of the brake and caliper.

front end and caliper. Individual parts were drawn to the correct dimensions and then mated in an assembly, thus defining the part's relationships and degrees of freedom.

Figure 2 shows the assembly was precisely dimensioned, as the machined design was to be a direct carbon copy of the 3D model. This design went through many

iterations until the design looked feasible enough to be built and tested.

3.3 Static analysis

A static structural evaluation comprises an examination of the structure's deflection, forces, strains, and stress as a result of applied load. Static structural analysis is required for pre-stressed modal evaluation. When an area is explained in terms of the instantaneous dimensions of a specimen, i.e., its actual area, the stress equation is provided by Eq. (1), strain equation is defined in Eq. (2), and the safety factor is defined in Eq. (3), as shown below [23]:

Stress equation

$$\sigma = \frac{F}{A}, \quad (1)$$

where σ = stress (MPa), F = applied force (N), and A = cross-sectional area (mm^2).

Strain equation

$$\varepsilon = \ln \frac{l_i}{l_0}, \quad (2)$$

where ε = true strain (mm/mm), l_0 = original length (mm), and l_i = deformed length (mm).

Safety factor equation

$$\text{FoS} = \frac{\sigma_y}{\sigma}, \quad (3)$$

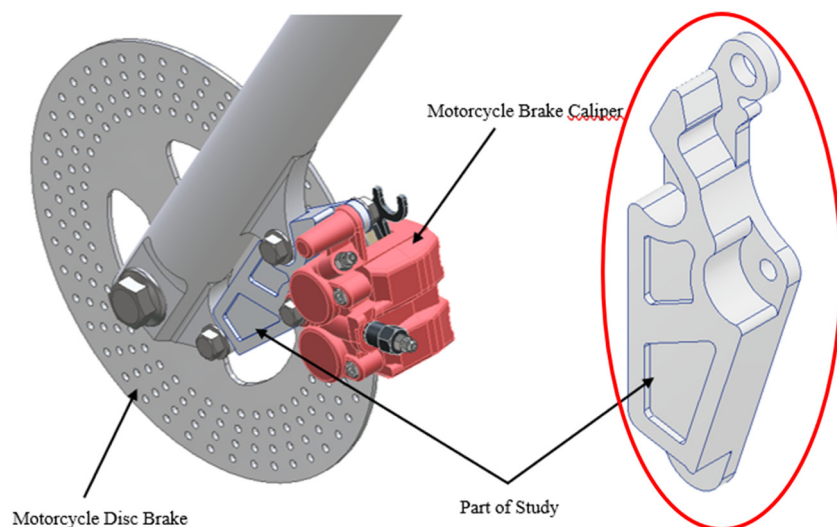


Figure 2: Object analysis.

where FoS = Factor of Safety (dimensionless), σ_y = yield strength (MPa), and σ = working stress (MPa).

3.4 Finite element formulation

Finite element analysis (FEA) is a numerical method for solving complex structural problems by discretizing a continuum domain into a finite number of elements. In this study, the bracket geometry was discretized using tetrahedral elements with three translational degrees of freedom per node. The fundamental equation governing the structural analysis in FEA is the global equilibrium equation:

$$[K]\{u\} = \{F\}, \quad (4)$$

where $[K]$ is the global stiffness matrix (N/mm), $\{u\}$ is the nodal displacement vector (mm), and $\{F\}$ is the external nodal force vector (N).

Eq. (4) enables the evaluation of structural responses such as deformation and stress distribution under specific boundary conditions. The method applied in this study follows the standard finite element formulation, as described by Rugarli [24].

4 Finite element method

The best software tool for tackling various engineering problems accurately enough is FEA. Numerous engineering problems are examined using the FEA, which discretizes complicated forms or complex areas that form a continuum into simple geometrical shapes.

In this study, the FEA method was employed using Ansys software to investigate the structural behavior of the components under study. Ansys provided a robust platform for creating accurate computational models of physical structures, allowing for detailed analysis of stress distribution, deformation characteristics, and overall performance under various loading conditions. The FEA simulations conducted in Ansys facilitated a comprehensive evaluation of the structural integrity and performance optimization strategies, essential for advancing the understanding and design refinement of the studied components.

Existing mathematical tools cannot handle intricate or convoluted forms in current mechanical design, which is frequently constructed of many materials. The FEA must be used by engineers to assess their designs. The process of breaking down a complex form model into smaller components is known as meshing. Each component's behavior under every conceivable support and load situation is fully known. The analytical process is shown in Figure 3.

4.1 Meshing of tetrahedral structural solid

The three categories of FEA elements are 1D elements, 2D elements, and 3D elements. Their shapes help us identify them. Elements can be in the form of a tetrahedron, a triangle, a quadrilateral, a straight line, a curve, and many more forms. The most fundamental component is a line with two nodes. Since all straight and curved line elements include translational and rotational displacement functions, they are all categorized as 1D elements [13]. Examples of 1D elements are beam and truss elements [24–26].

Frequently, 3D parts are used to mesh volumes. When an issue cannot be simplified, they are used and produced from 2D elements [25]. 3D solid components only take into account translational displacements. The three translational unknown

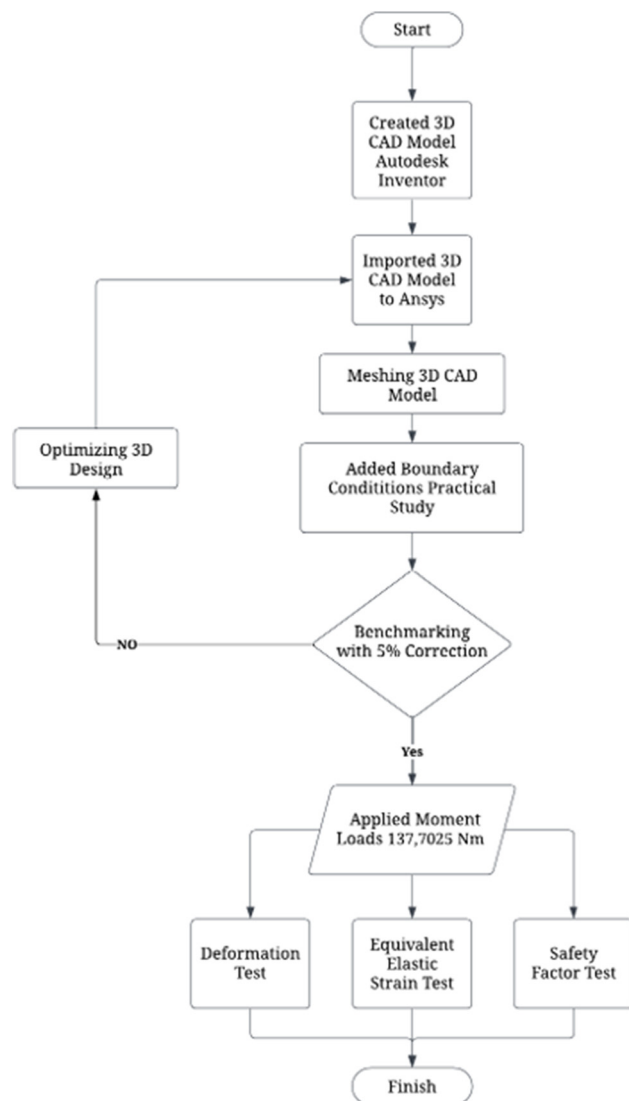


Figure 3: Finite element analysis process.

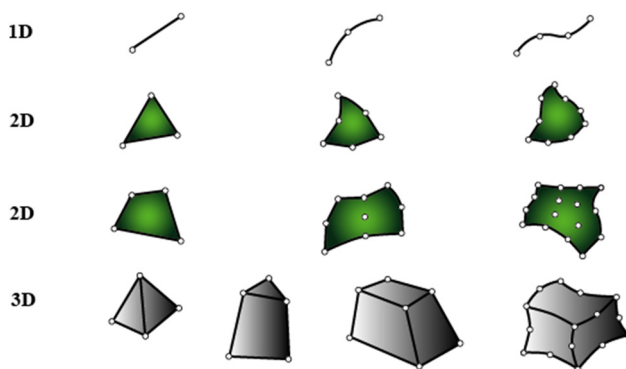


Figure 4: Typical finite element geometries.

displacement functions are $u(x, y, z)$, $v(x, y, z)$, and $w(x, y, z)$ [9,10]. Examples of 3D solid elements include the 4-node tetrahedral element, the 10-node tetrahedral element, the 8-node isoparametric element, and others, as shown in Figure 4.

In this study, a mesh size of 1.5 mm is used and the type of element is tetrahedral. With a 1.5-mm mesh size, the area of the bracket caliper is divided into consistent-sized elements, allowing for more accurate simulations. With a smaller mesh size, the discretization elements are denser, enabling more detailed and accurate modeling of the structural bracket response. Larger mesh sizes may reduce computation time but may sacrifice accuracy and resolution in representing the structural model's response.

4.2 Boundary conditions and material selection

In this research, there are two points, namely the fixed support and the moment shown in Figure 5. The fixed

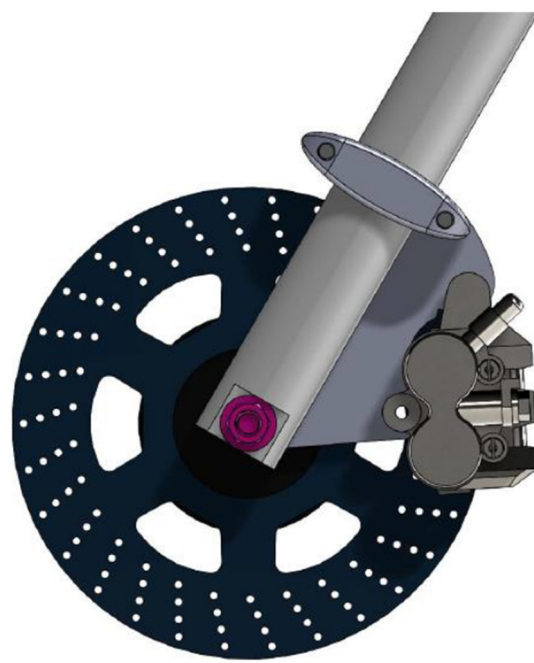


Figure 6: Problem definition [27].

support is defined at the mounting holes of the bracket (Point A), restricting all degrees of freedom. A moment load of 137 Nm is applied at Point B, simulating the braking force transmitted to the bracket during deceleration. These conditions reflect realistic operational conditions for a motorcycle front brake system.

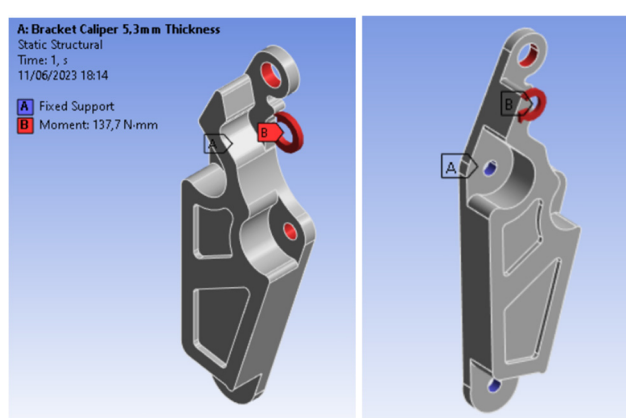


Figure 5: The Point A as fixed support location.

Table 3: Benchmark result of present study with practical study

Mesh size (mm)	Element	Deformation		Correction (%)
		Present study	Practical	
1	1505208	0.035015	0.03411	2.65
1.25	787795	0.035012	0.03411	2.64
1.5	452009	0.035096	0.03411	2.89
1.75	285669	0.035089	0.03411	2.87
2	180138	0.035078	0.03411	2.84
2.25	129446	0.035063	0.03411	2.79
2.5	103142	0.035042	0.03411	2.73
3	56902	0.035013	0.03411	2.65
3.25	48141	0.034988	0.03411	2.57
3.5	35069	0.03493	0.03411	2.40
3.75	25613	0.034945	0.03411	2.45
4	27554	0.034818	0.03411	2.08
5	11823	0.03466	0.03411	1.61
6	6152	0.03433	0.03411	0.64
7	4364	0.034168	0.03411	0.17
8	3335	0.033926	0.03411	-0.54

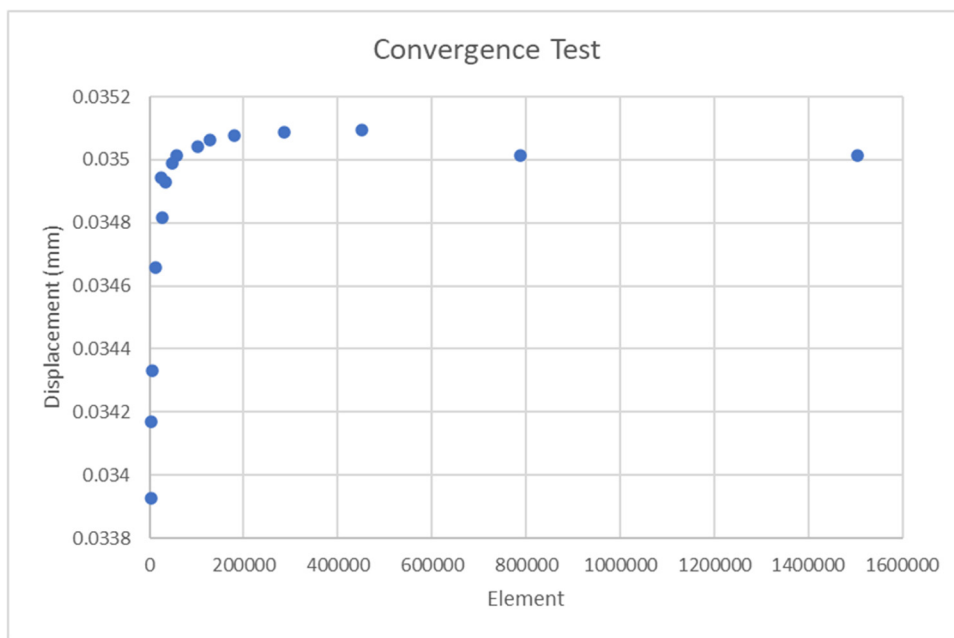


Figure 7: Mesh convergence test.

5 The benchmark study and convergence test

In the study by Mat Pekin [27] in Figure 6, validation was conducted to ensure that the bracket meets the required performance and expected criteria. The previous research provided validation criteria that the bracket design must meet. These criteria include Deformation and Equivalent Elastic Strain. The validation results are shown in Table 3, where the deformation and Equivalent Elastic Strain values meet the specified correction below 5%.

The design validation has significant implications for the development of improved caliper brackets. The validation results are also relevant in supporting design decisions and selecting the appropriate material for the caliper bracket to be used in broader applications.

To determine the optimal mesh size for our specific problem, we conducted a mesh convergence test. The primary objective was to assess how the displacement field converges as we refine the mesh as shown in Table 3.

The convergence test revealed that beyond a certain number of elements, further mesh refinement did not significantly affect the displacement results. Specifically, the displacement values reached a plateau, indicating that the mesh had converged. Based on this analysis, we confidently selected a mesh size of 1.5 mm for subsequent simulations, as shown in Figure 7, and the detail mesh can be seen in Figure 8.

6 Static structural analysis of the bracket caliper

In a different scenario, a different loading is used. Based on the research conducted by Gusniar and Ibrahim in 2021 [28], it was found that the Honda Beat Sporty 2017 vehicle requires a braking force of 1101.62 N to come to a complete stop within a braking time of 4.94 s. This friction force will be implemented in the numerical model. The result for deformation and equivalent are as follows:

Figure 9 presents the comparison of two materials: cast iron (EN-GJL-100) and aluminum alloy, wrought, 6061 T6. Cast iron exhibits a total deformation of 0.00015598 and an equivalent elastic strain of 0.0000016222 mm/mm, as shown in Figure 10, while aluminum alloy has a total deformation of 0.00020265 mm and an equivalent elastic strain of 0.0000020841 mm/mm as shown in Figure 10. Considering these mechanical properties, cast iron is preferable for applications requiring durability and strength under heavy loads or extended periods due to its superior ability to withstand higher strains without permanent deformation.

7 Topology optimization

In the optimization process, constraints are also given by providing the optimum model with a minimum limit value of 0.5% of the original mass weight. The constraints were

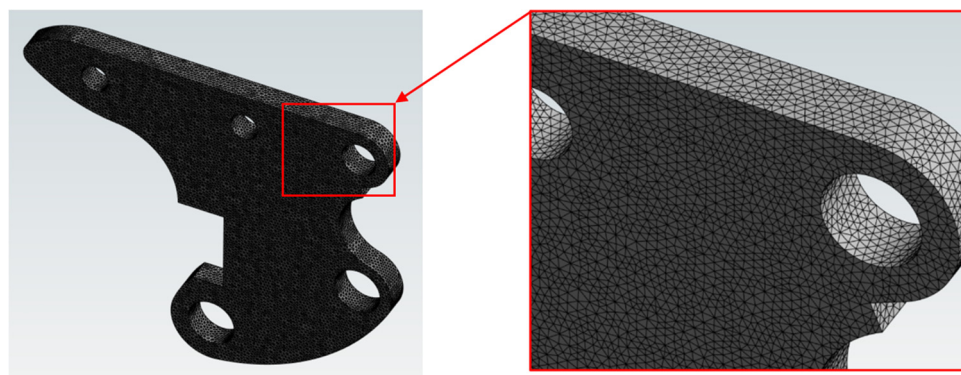


Figure 8: Detail of mesh size 1.5 mm with 4,52,009 elements.

adjusted for the initial model to meet the constraints. After that, the optimization process can be run by giving the command a limit on the iteration time. It should be noted that topology optimization achieves convergence values in the range of iteration time. The optimization process stops when the minimum strain value is obtained until it converges. In Table 4, the structural assessment phase is repeated by incorporating several optimized frames into a complete bracket structure.

Topology optimization is a method that utilizes computers to determine the optimal arrangement of materials within a design space, considering loads, boundary conditions, and other constraints. In this study, the objective function is based on minimizing compliance. Eq. (5) shows how to write the objective function mathematically:

$$\min(x)c(u) = \frac{1}{2}u^T Ku, \quad (5)$$

where $c(u)$ is the total compliance of the structure, u is the global displacement vector, and K is the global stiffness matrix, which depends on the material distribution x .

The goal of this formulation is to obtain the stiffest possible structure by minimizing the strain energy under static loading, while satisfying the governing equilibrium (Eq. (5)):

$$K(x)u = F \quad (6)$$

subject to a volume constraint:

$$\frac{V(x)}{V_0} \leq f, \quad (7)$$

where $V(x)$ is the current material volume, V_0 is the initial total design volume, and f is the prescribed volume fraction.

This formulation is based on the solid isotropic material with penalization method, which punishes intermediate density values to encourage a binary (0–1) material distribution. Using Eq. (7) ensures that the resulting structure is as stiff as possible while using the least amount of material. The literature has made extensive use of this approach and formulation, including in the work of Andreozzi and Davino [18].

The combined objective convergence criterion in Figure 11 shows a decrease in the objective function and

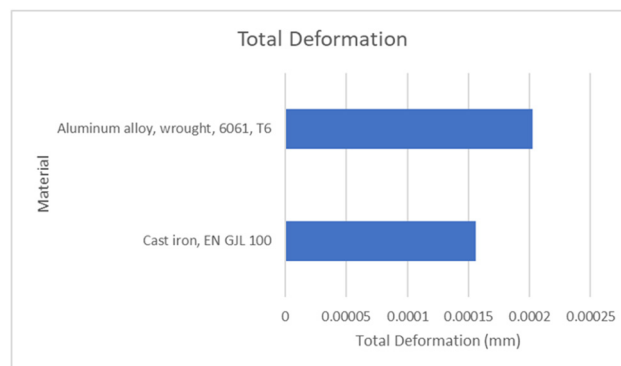


Figure 9: Total deformation analysis result of aluminum alloy, wrought, 6061 T6 and cast iron, EN GJL 100.

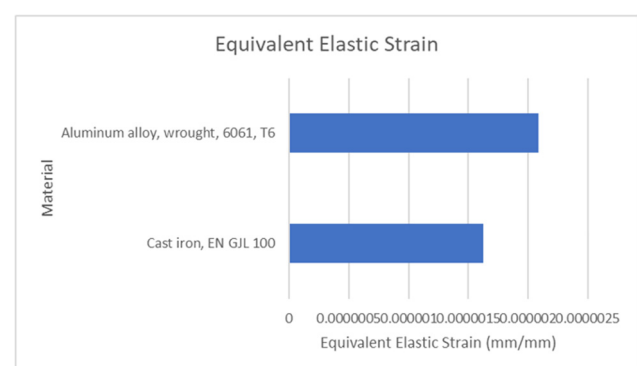


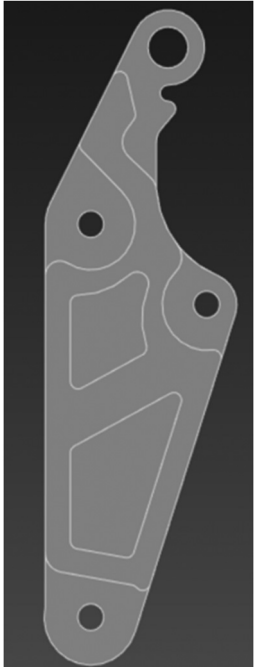
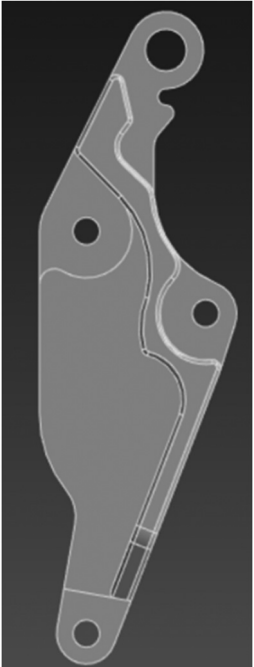
Figure 10: Equivalent elastic strain analysis result of aluminum alloy, wrought, 6061 T6 and cast iron, EN GJL 100.

constraint violation across iterations. The mass response criterion graph demonstrates mass reduction with each iteration obtained from the Ansys software, emphasizing early efficiency gains, as shown in Figure 12.

Table 5 shows the comparison of the initial and optimized results for three mechanical properties: deformation, strain, and stress. The optimization reduced deformation by 15%. Strain

decreased by 21% after optimization. Stress experienced a 25% reduction due to optimization. In this specific topology, weight reduction occurs consistently, resulting in a 31% decrease. The details of the Global FEA result after optimization can be seen in Table 6. It can be concluded that the topology optimization is effective to evaluate the analysis of the bracket for reducing the value of deformation, strain, and stress by using FEA.

Table 4: Summary of optimization result

Before	After
	
	

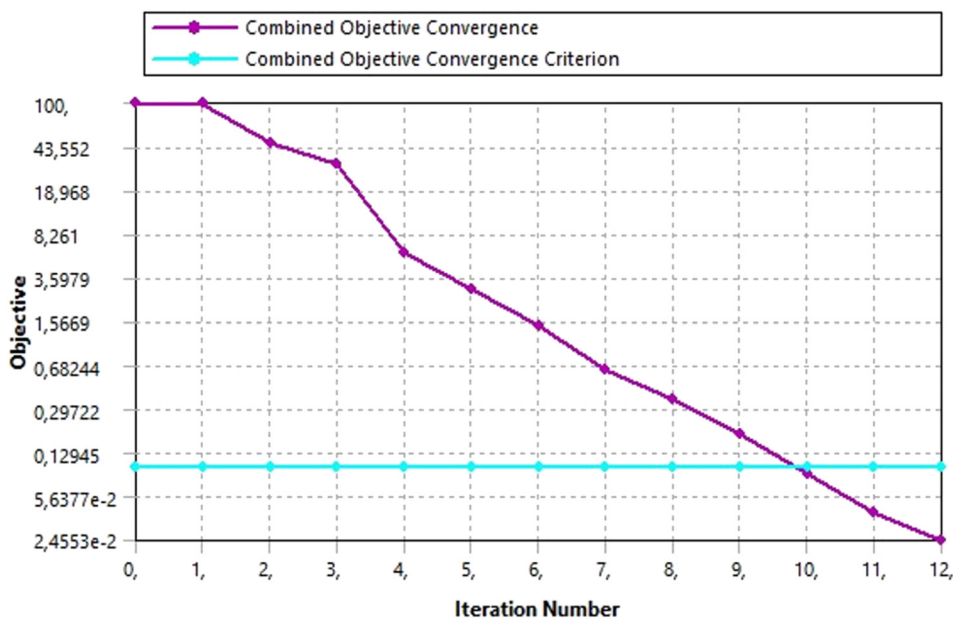


Figure 11: Combined objective convergence criterion.

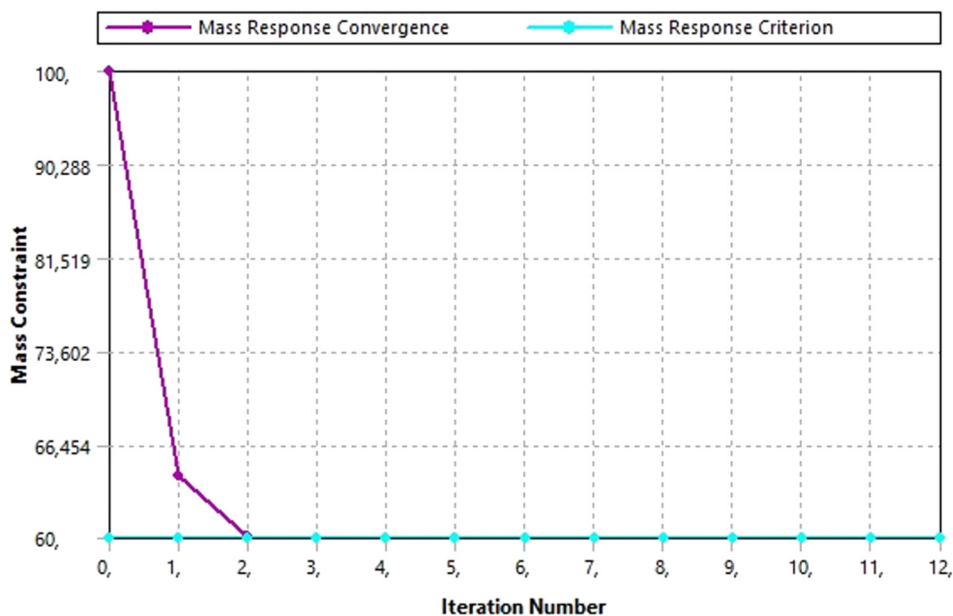
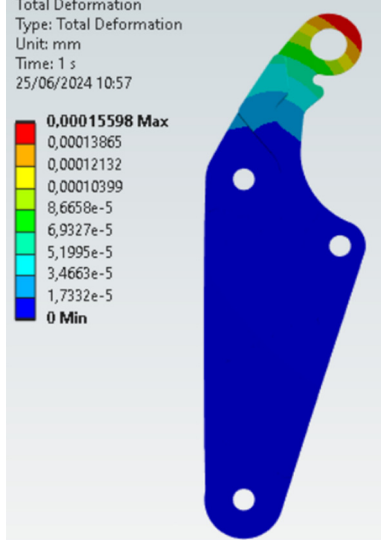
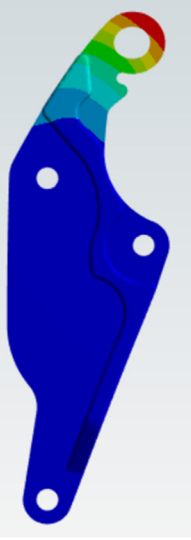
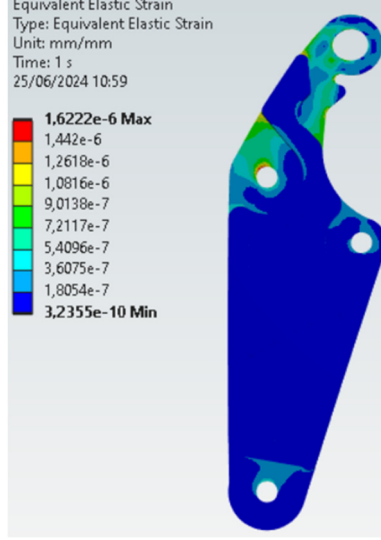
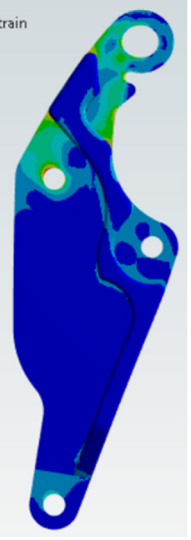
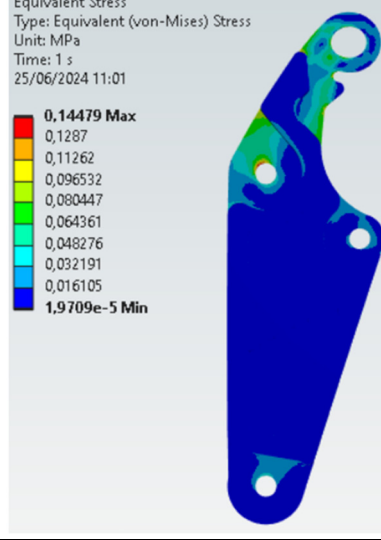
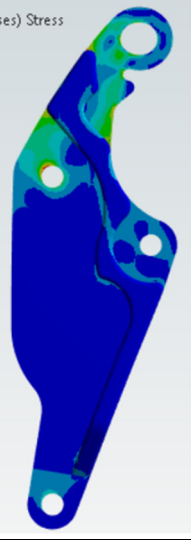


Figure 12: Iteration combined objective convergence criterion and mass response criterion.

Table 5: Mechanical properties and weight loss table

Analysis	Result		Mechanical properties loss (%)	Weight (kg)		Weight loss (%)
	Initial	Optimized		Initial	Optimized	
Deformation (mm)	1.56×10^{-4}	1.33×10^{-4}	15	0.65886	0.4573	31
Strain (mm/mm)	1.62×10^{-6}	1.28×10^{-6}	21	0.65886	0.4573	31
Stress (MPa)	0.15259	0.11428	25	0.65886	0.4573	31

Table 6: Global FEA result after optimization

	Before	After
Deformation (mm)	<p>Total Deformation Type: Total Deformation Unit: mm Time: 1 s 25/06/2024 10:57</p>  <p>0.00015598 Max 0,00013865 0,00012132 0,00010399 8,6658e-5 6,9327e-5 5,1995e-5 3,4663e-5 1,7332e-5 0 Min</p>	<p>Total Deformation Type: Total Deformation Unit: mm Time: 1 s 25/06/2024 10:51</p>  <p>0.0001329 Max 0,00011813 0,00010337 8,8599e-5 7,3832e-5 5,9066e-5 4,4299e-5 2,9533e-5 1,4276e-5 0 Min</p>
Equivalent elastic strain (mm/mm)	<p>Equivalent Elastic Strain Type: Equivalent Elastic Strain Unit: mm/mm Time: 1 s 25/06/2024 10:59</p>  <p>1.6222e-6 Max 1,442e-6 1,2618e-6 1,0816e-6 9,0138e-7 7,2117e-7 5,4096e-7 3,6075e-7 1,8054e-7 3.2355e-10 Min</p>	<p>Equivalent Elastic Strain Type: Equivalent Elastic Strain Unit: mm/mm Time: 1 s 25/06/2024 11:00</p>  <p>1.2816e-6 Max 1,1392e-6 9,9688e-7 8,5452e-7 7,1215e-7 5,6979e-7 4,2742e-7 2,8506e-7 1,4269e-7 3,2873e-10 Min</p>
Equivalent (von-misses) stress	<p>Equivalent Stress Type: Equivalent (von-Mises) Stress Unit: MPa Time: 1 s 25/06/2024 11:01</p>  <p>0,144479 Max 0,1287 0,11262 0,096532 0,080447 0,064361 0,048276 0,032191 0,016105 1,9709e-5 Min</p>	<p>Equivalent Stress Type: Equivalent (von-Mises) Stress Unit: MPa Time: 1 s 25/06/2024 11:01</p>  <p>0,11428 Max 0,10159 0,088894 0,076199 0,063504 0,050809 0,038114 0,025419 0,012724 2,9252e-5 Min</p>

8 Conclusions

In this study, the bracket caliper was tested using FEA using two different types of materials: aluminum alloy, wrought, 6061 T6 and cast iron EN GJL 100. Before conducting the analysis, the benchmarking study was conducted by mesh selection and analysis for the convergence study. The validation result indicates that the present study, when compared to the previous study, shows an error of less than 5%, confirming that the selected parameters are valid for performing static analysis using FEA.

During the static analysis, the bracket caliper was given a momentum of 137.7 Nm. Based on the results of the analysis, it can be seen that cast iron material has a maximum deformation result and a smaller elastic strain equivalent compared to the aluminum alloy, wrought, 6061 T6 material. As for the safety factor, the cast iron EN GJL 100 material has a higher safety factor value than the alloy 6061 T6. Thus, it can be concluded that the cast iron material EN GJL 100 has better deformation, elastic equivalent, and safety factor than the aluminum alloy, wrought, 6061 T6 material. For further research, other parameters can be explored to maximize the bracket caliper design and achieve its best possible configuration.

On the other hand, the topology optimizations have been done for this study. The studies compare initial and optimized results for three mechanical properties: deformation, strain, and stress. The optimization reduced deformation by 15%. Strain decreased by 21% after optimization. Stress experienced a 25% reduction due to optimization. In this specific topology, weight reduction occurs consistently, resulting in a 31% decrease. Thus, the topology optimization is effective to evaluate the analysis of the design structure such as bracket caliper.

Further studies are recommended to investigate the effects of varying material properties and boundary conditions in FEA models using Ansys. Such investigations would provide a more comprehensive understanding of how these variations influence the overall structural behavior and performance under diverse scenarios. By incorporating different materials and boundary constraints into the FEA simulations, future research can help generalize the findings and enhance the predictive accuracy of the models. This approach will allow researchers to address a broader range of engineering problems, improving the robustness and applicability of FEA results in real-world applications. Additionally, exploring these aspects can contribute to the development of more versatile and resilient design strategies, ultimately leading to more optimized and reliable engineering solutions.

Acknowledgments: The authors wish to thank the Department of Mechanical Engineering, Universitas Negeri Semarang, for the use of facilities in their laboratories.

Funding information: The authors state no funding involved.

Author contributions: All authors have accepted responsibility for the entire content of this manuscript and consented to its submission to the journal, reviewed all the results, and approved the final version of the manuscript. Conceptualization: A.B., A.A.G., S.A., and D.F.F. Methodology: A.B., A.A.G., and R.D.W. Software: S.W.L., J.H.C., and T.M. Validation: J.P.S. and T.C. Formal analysis: J.M. and A.Y.M. Writing – draft, review, and editing: A.B. and A.A.G. Supervision: A.B. and A.A.G.

Conflict of interest: The authors state no conflict of interest.

Data availability statement: The data supporting the findings of this study are available from the corresponding author upon reasonable request.

References

- [1] Wu SR, James C. Advanced development of explicit FEA in automotive applications computer methods in applied mechanics and engineering. *J Educat Tech.* 1997;149:189–99.
- [2] Kamal M, Rahcman MM, Rahman AGA. Finite element application in mechanical structure evaluation. *J Mech Sci.* 2012;3:291–300.
- [3] Kamal M, Rahman MM, Rahman AGA. Numerical simulation of automotive structural components using FEA. *Inter J Automot Mech Eng.* 2013;7:912–23.
- [4] Mahendra M. Applications of finite element analysis in structural engineering. In: *Proc Int Conf Comput Aided Eng.* 2007. p. 38–46.
- [5] Zulkifli A, Ariffin AK, Rahman MM. Finite element analysis in automotive design applications. *Inter J Automot Mech Eng.* 2011;3:256–64.
- [6] Daud R, Ariffin AK, Abdullah S. Fatigue life prediction using FEA approach in automotive components. *Inter J Automot Mech Eng.* 2013;7:995–1006.
- [7] Huzni S, Ilfan M, Sulaiman T, Fonna S, Ridha M, Arifin AK. Structural behavior of automotive components using finite element analysis. *Inter J Automot Mech Eng.* 2013;7:1023–30.
- [8] Newberry AL. FEA modeling proves its worth in composite design in RP Asia. Conf. Held at Kuala Lumpur Malaysia. 2000-09-20.
- [9] Kardigama K, Rahman MM, Ismail AR, Bakar RA. Numerical modelling for composite components using FEA. *J Mech Eng Sci.* 2020;1:37–66.
- [10] Najiha MS, Rahman MM, Yusoff AR, Kardigama K. Finite element investigation on mechanical components for stress evaluation. *Inter J Mech Eng.* 2021;6:766–44.
- [11] Colorado D. Introduction to finite element methods (ASEN 5007) Ch. 6 FEM modelling: introduction. Online resource, accessed: Jun. 2023. Available: <http://www.colorado.edu/engineering/cas/courses.d/>.

- [12] Logan DL. *A first course in the finite element method*. 4th ed. Canada: Thomsom Canada Limited; 2007.
- [13] Berlioz T. *Solid mechanics using the finite element method*. USA: John Wiley & Sons Inc; 2010.
- [14] Ma G, Zhou J. Finite element analysis of an ammunition bracket. Wuhan: Wuhan University Press; 2021.
- [15] Prunier F, Branque D. Definition of a safety factor using the finite element method in geomechanics, from a static to dynamic regime. *Europ J Environ Civil Eng*. 2019;26:144–65.
- [16] Wibawa LAN. Pengaruh Pemilihan Material Terhadap Kekuatan Rangka Main Landing Gear Untuk Pesawat UAV. *Jurnal Teknologi Dan Terapan Bisnis*. 2019;2(1):48–52.
- [17] Sóbestér A, Keane A, Scanlan J, Bressloff N. Conceptual design of UAV airframes using a generic geometry service. *InInfotech@ Aerospace*. 2005-09;26–9.
- [18] Andreozzi A, Davino D. Topological sensitivity analysis and its applications. *Adv Eng Softw*. 2015;86:12–25.
- [19] Guo L, Liu Y. Topology optimization for additive manufacturing considering manufacturing constraints. *Struct Multidiscipl Optim*. 2018;57:1427–43.
- [20] Liu J, Zhang X. Topology optimization with structural integrity constraints. *Struct Multidiscipl Optim*. 2019;60:879–93.
- [21] Zhou M, Wang Q. Topology optimization for sustainable design. *J Clean Prod*. 2020.
- [22] Matweb. MatWeb, Your source for materials information. *MatWeb*. 2015;1–2.
- [23] Pelleg J. *Mechanical properties of materials*. Springer; 2013. Vol. 190. doi: 10.1007/978-94-007-4342-7.
- [24] Rugarli. *Structural analysis with finite elements*. UK: Thomas Telford Limited; 2010.
- [25] Boeraeve P. *Introduction to the finite element method*. Accessed: Jun. 2023. Liège: Institut Gramme; www.gramme.be/unite9/FEM/FiniteElementMethod.pdf.
- [26] Papadupulos. *Introduction to Finite Element Method*. Accessed: Jun;2023. Available: www.kochmann.caltech.edu/ae108a/FEnotes.pdf.
- [27] Pekin M. *Design and construction of a motorcycle drum to disc*. Kuala Lumpur: University of Malaysia Press; 2020.
- [28] Gusniar IN, Ibrahim SA. *Analisis Gaya pada Rem Cakram (Disk Brake) pada Kendaraan Roda Dua (Honda Beat Sporty 2017*. *Jurnal Pendidikan Teknik Mesin*. 2021;8(2):110–20.